

# Thermoplastic elastomers-based natural rubber and thermoplastic polyurethane blends

Skulrat Pichaiyut · Charoen Nakason ·  
Norbert Vennemann

Received: 11 July 2011 / Accepted: 26 October 2011 / Published online: 3 January 2012  
© Iran Polymer and Petrochemical Institute 2011

**Abstract** Thermoplastic elastomers based on the blends of thermoplastic polyurethane (TPU) and natural rubber were prepared by a simple blend technique. The influence of the two different types of natural rubber (i.e., unmodified natural rubber (NR) and epoxidized natural rubber (ENR)) on properties of the blends was investigated. The main aim of this study was to improve heat resistance and damping properties, and also to prepare the TPU material with low hardness by blending with various amounts of natural rubber. It was found that the TPU/ENR blends exhibited superior modulus, hardness, shear viscosity, stress relaxation behavior and heat-resistant properties compared to the blends with TPU and unmodified NR. This was attributed to higher chemical interaction between the polar functional groups of ENR and TPU by improving the interfacial adhesion. It was also found that the ENR/TPU blends exhibited finer grain morphology than the blends with unmodified NR. Furthermore, lower tension set, damping factor ( $\tan \delta$ ) and hardness, but higher degradation temperature, were observed in natural rubber/TPU blends compared to pure TPU. This proves the formation of TPU material with high heat resistance, low hardness and better damping properties. However, the blends with higher proportion of natural rubber exhibited lower tensile strength and elongation at break.

**Keywords** Thermoplastic elastomer · Thermoplastic polyurethane · Epoxidized natural rubber · Relaxation behavior · Simple blends

## Introduction

Thermoplastic elastomer (TPE) is a new class of material and probably the fastest growing sector in the polymer market [1]. TPEs based on the blend of rubber and thermoplastics have received considerable attention in recent years due to their relatively low cost of manufacturing with high potential plastic processing equipment. Typically, TPEs exhibit elastic and mechanical properties of rubber with the processing characteristics of thermoplastic materials. They have gained more importance because of their wide range of engineering applications in various fields, such as automotive parts, household appliances, electrical equipments, industrial supplies and medical apparatus [2]. Interest in TPE or thermoplastic natural rubber (TPNR) has increased recently due to green and environmental friendly behavior of the renewable natural rubber (NR) materials with some unique properties. A number of research reports are available in the literature on the preparation of TPNRs, which focus on blending of NR with various types of thermoplastics including high-density polyethylene [3], linear low-density polyethylene [4], polypropylene [5], polystyrene [6] and PMMA [7]. In some cases, chemical modification of NR molecules is performed for the preparation of TPNR materials. Epoxidized natural rubber (ENR) is one of the most frequently used modified NR to prepare TPNR by blending with various types of thermoplastics such as HDPE [8, 9] and PP [10, 11]. This is attributed to the superior properties, such as oil resistance, gas impermeability, good wet grip and high damping

S. Pichaiyut · C. Nakason (✉)  
Faculty of Science and Technology, Center of Excellence  
in Natural Rubber Technology, Prince of Songkla University,  
Pattani 94000, Thailand  
e-mail: ncharoen@bunga.pn.psu.ac.th

N. Vennemann  
Faculty of Engineering and Computer Science,  
University of Applied Sciences, Osnabrück, Germany



characteristics of ENR. Polymer blends were also prepared by blending ENR with polar thermoplastics, such as copolymer of ethylene vinyl acetate (EVA) [12], poly(vinyl chloride) [13] and poly(methyl methacrylate) [14, 15]. Apart from TPNR, TPE materials prepared by various types of blending pairs of synthetic rubber and thermoplastics have been widely investigated. These include PP/EPDM [16, 17], LDPE/EPDM [18] and NBR/PVC [19, 20] blends.

Thermoplastic polyurethane (TPU) is a class of polymer with a number of useful properties, including excellent abrasion resistance, outstanding low-temperature performance, excellent mechanical properties, good tear strength, high elasticity and high transparency together with good resistance toward oil and grease. Technically, TPU is a TPE material consisting of linear segmented block copolymers composed of hard crystalline phase and soft amorphous segments. The currently available TPU can be divided mainly into two groups based on soft segment structures: polyester-based and polyether-based TPUs. Polyester-based TPU is typically a general purpose material, while the polyether-based TPU is applicable when excellent hydrolysis, microbial resistance as well as extreme low-temperature flexibility is required. A light color TPU with non-yellowing performance was prepared by using aliphatic isocyanates [21]. By variations in the content of hard and soft phases, the properties of TPU can be adapted easily to their respective applications. The hard segments are connected by intermolecular hydrogen bonds and form crystalline domain to act as physical cross-links and reinforcing fillers, while the soft segments form an elastomer matrix which accounts for the elastic properties of TPU [22]. Blending of TPU with other polymers has been of considerable interest in recent years. Polypropylene (PP) is one of the most frequently used components to blend with TPU [23–25]. The main aim has been to reduce cost, improve thermal stability and promote the blend compatibility. TPU has been used to blend with various polar thermoplastics including functionalized polypropylene [26], polyamide-12 [27], polyamide-10 [28], poly(butylene terephthalate) [29], poly(vinylidene fluoride) [30], PVC [31, 32], maleic-anhydride grafted polyethylene [33] and copolymer of styrene and acrylonitrile (SAN) [34, 35]. The TPU has also been used to prepare the novel TPE by blending with epoxidized NR with 25 mol% epoxide groups (ENR-25) in our previous work [36]. The main aim was to study the influence of two different types of blending techniques (i.e., simple blending and dynamic vulcanization) on the properties of ENR-25/TPU blends.

Typically, TPUs with low hardness exhibit poor mechanical properties and they are not suitable for engineering applications. Additionally, one of the main disadvantages of TPU material is the damping behavior, which is significantly higher compared to the conventional

elastomeric material, in particular to that of NR. In contrast, NR exhibits excellent mechanical properties even at low hardness and also unattainable low damping properties under conditions of dynamic loads. Hence, blending of TPU and NR may result in materials with outstanding performance, especially at low hardness. Because of compatibility reasons and to increase oil and heat resistance of the blends, modified NR in the form of ENR was used instead of simple unmodified NR. Therefore, in this work, ENR and TPU blends were prepared by a simple blend technique (i.e., without curatives). For comparison, the unmodified NR (i.e., air-dried sheet, ADS) was also used to blend with TPU. The dynamic mechanical, rheological, thermal, morphological and stress relaxation properties of the blends were investigated.

## Experimental

### Materials

Two types of NR were used in this study: air-dried sheet (ADS) of unmodified NR and ENR. The ADS was purchased from a local factory operated by Khuan Pan Tae Farmer Cooperation (Phattalung, Thailand). The epoxidized NR with 50 mol% epoxide (i.e., ENR-50) was prepared in-house using high ammonia (HA) concentrated NR latex (manufactured by Yala Latex, Yala, Thailand) with a dry rubber content of approximately 60%. In situ performic epoxidation of formic acid (manufactured by Riedel-de Haen, Seelze, Germany) and hydrogen peroxide (manufactured by Riedel-de Haen, Seelze, Germany) was performed by preparation and characterization procedures, which are described elsewhere [37]. Aliphatic polyester-based TPU, Elastollan<sup>®</sup> LP 9273 was used as the thermoplastic blend component. It was manufactured by Elastogran GmbH, Lemförde, Germany, with specific gravity of 1.14 g/cm<sup>3</sup>, melting temperature of 160 °C and hardness of 84 Shore A. A polyphenolic antioxidant additive, Wingstay L, was manufactured by Eliokem, OH, USA.

### Preparation of natural rubber/TPU blends

TPU was first dried at 80 °C for 2 h. A two-step mixing process was then performed. First, NR and antioxidant (i.e., Wingstay L) were mixed by using a Haake Rheocord 600 laboratory internal mixer (Thermo Electron Corporation, Karlsruhe, Germany) at 80 °C with a rotor speed of 40 rpm and a mixing time of 4 min. The rubber mix was then removed from the mixer and cooled down to room temperature. In the second step, the rubber mix was incorporated into the internal mixer and mixed at 145 °C at a rotor speed of 80 rpm for 0.5 min, and then the rotor speed was

increased to 150 rpm for another 0.5 min. After reaching a temperature of approximately 140–145 °C, the TPU was added. Then, the temperature of the blend was gradually raised to a temperature range of 166–175 °C due to the frictional heat. The rotor speed was then dropped to 60 rpm to reduce the mixing temperature and mixing was continued for another 7 min (i.e., with the total mixing time of approximately 8 min). The blend product was finally removed from the mixer, cooled down to room temperature and cut into small pieces. The test specimens were then prepared by injection molding technique.

#### Rheological characterization

High pressure capillary rheometer (Göttfert Rheo-Tester 2000 GmbH, Buchen, Germany) was used to follow shear flow properties of the blends. The dimensions of the capillary die used was 1-mm diameter, 20-mm length and 180° entry angle with an aspect ratio ( $L/D$ ) of 20/1. The test was carried out at a wide range of shear rate ( $10$ – $2,000\text{ s}^{-1}$ ) with a test temperature of 220 °C. During the test, the dried material was first incorporated into the rheometer's barrel and left for 5 min to allow the material to melt. The molten material was then continuously purged through the capillary die until it reached a pressure of approximately 100 MPa with the help of pistons. This was to eliminate bubbles formed in the melt and to obtain a compact mass in the barrel. The pressure was then allowed to drop to approximately 5–10 MPa and then pre-conditioned for at least 5 min before commencing the test. The test was then carried out with a set of shear rates in a program via microprocessor. The pressure drop across the capillary channel and melt temperature was captured via data acquisition systems. In this work, the apparent values of shear stress, shear rate and shear viscosity were calculated using a derivative of the Poiseuille law for capillary flow, as described in literature [38].

#### Mechanical testing

Tensile testing of samples was performed at  $23 \pm 2$  °C according to ISO 527 using Zwick Z 1545 tensile test machine (Zwick GmbH & Co., Ulm, Germany) at a fixed extension speed of 200 mm/min. The dumbbell-shaped specimens were first prepared by a thermoplastic injection molding machine (Babyplast type 6/10P-Tmicro-molding machine, Cronoplast, S.L. Barcelona, Spain). The tension set at 100% elongation was also determined at room temperature ( $23 \pm 2$  °C) according to ISO 2285. The samples were kept under tension for a fixed elongation of 100% and time interval of 10 min. Dimensions of the samples were then determined compared to their original shapes.

Indentation hardness was tested by using a Shore A durometer (Frank GmbH, Hamburg, Germany) according to ISO 868.

#### Dynamic properties

Dynamic properties were characterized by using a rotorless oscillating shear rheometer (Rheo tech MDPT, Cuyahoga Falls, USA) at 180 °C. The oscillation frequency was set in the range of 0.6–95 rad/s at a constant strain of 3% to assure the test was in the range of linear viscoelasticity. The elastic modulus ( $G'$ ) and damping factor in terms of  $\tan \delta = G''/G'$  of the blends were characterized, where  $G'$  is the elastic modulus and  $G''$  is the loss modulus.

#### Temperature scanning stress relaxation (TSSR)

The TSSR measurement was performed using the TSSR instrument (Brabender GmbH, Duisburg, Germany). The instrument consists of an electrical heating chamber where the sample was placed between two clamps, which were connected to a linear drive unit to apply a certain uniaxial extension to the sample. A high-quality signal amplifier in combination with a high-resolution AD-converter was used to detect and digitize analog signals of the high-resolution force transducer and transferred to a personal computer. A special software program was used to treat and evaluate the data as well as to control the machine system. In this study, the dumbbell-shaped specimens (type 5A, ISO 527) were used. The sample was first conditioned at room temperature (i.e.,  $23 \pm 2$  °C) for 2 h. Then, the sample was clamped in the chamber of TSSR instrument and a fixed extension of 50% was applied. A constant heating rate of 2 K/min was then applied until the stress relaxation was complete or the sample ruptured. The applied forces or applied stresses (i.e.,  $F(T)/F_0$ ) at various testing temperatures were recorded in terms of force–temperature or stress–temperature curves. Furthermore, certain characteristics of the samples, such as  $T_{10}$ ,  $T_{50}$ ,  $T_{90}$  and the rubber index (RI), were calculated. It is noted that the temperature  $T_x$  stands for the temperature at which the force  $F$  has decreased by about  $x\%$  with respect to the initial force,  $F_0$ , while RI is a measure of rubber-like behavior of the material, calculated from the total area under the force–temperature curves according to the relation below [39, 40]:

$$RI = \frac{\int_{T_0}^{T_{90}} F(T)/F_0 dT}{T_{90} - T_0} \quad (1)$$

where  $F(T)$  is the force at testing temperature,  $T$ , and  $F_0$  is the initial force determined at a starting temperature ( $T_0$ ).  $T_{90}$  is the temperature at which the force,  $F$ , has decreased by about 90% with respect to the initial force ( $F_0$ ).



Furthermore, the relaxation spectrum,  $H'(T)$ , was calculated using the following equation [39]:

$$H'(T) = -T \left( \frac{dE(T)}{dT} \right)_{v=\text{const}} \quad (2)$$

$$E(T) = \sigma(T)/\varepsilon_0$$

where  $\sigma(T)$  is the temperature-dependent stress and  $\varepsilon_0$  is the applied strain (i.e., 50%).

### Thermal properties

Three techniques were used to characterize the thermal behavior of NR/TPU blends, namely thermogravimetric analysis (TGA), dynamic mechanical analysis (DMA) and differential scanning calorimetry (DSC). The TGA was performed using Perkin Elmer STA600 (New Shelton, USA). The samples were first placed in the platinum pan under a nitrogen atmosphere. The test was then performed with a heating rate of  $10\text{ }^\circ\text{C min}^{-1}$  in the temperature range of  $30\text{--}600\text{ }^\circ\text{C}$ . The DMA measurement was carried out on a Perkin Elmer DMA8000 (New Shelton, USA). The sample was heated at a heating rate of  $5\text{ }^\circ\text{C/min}$  in the temperature range of  $-100$  to  $180\text{ }^\circ\text{C}$  and a frequency of  $1\text{ Hz}$ . The DSC was performed using DSC-7 (Perkin Elmer, New Shelton, USA). The sample was first heated with a heating rate of  $10\text{ }^\circ\text{C/min}$  to  $180\text{ }^\circ\text{C}$  and left at this temperature for  $5\text{ min}$  to eliminate the thermal history. The samples were subsequently cooled down to  $-100\text{ }^\circ\text{C}$  with a cooling rate of  $10\text{ }^\circ\text{C/min}$ . The second heating was again performed from  $-100\text{ }^\circ\text{C}$  to  $170\text{ }^\circ\text{C}$  with a heating rate of  $10\text{ }^\circ\text{C/min}$ . The data were captured from the last run.

### Morphological properties

Morphological characterization was performed using scanning electron microscope (SEM) model JSM-5200 (Jeol Co., Tokyo, Japan) and atomic force microscopy (AFM) model Nanosurf<sup>®</sup> easyScan 2 AFM (Nanosurf AG, Liestal, Switzerland). In SEM characterization, the samples were first cryogenically cracked in liquid nitrogen to prevent any possibility of phase deformation. The rubber phase was then preferentially extracted by dissolving the fracture surface in toluene. The samples were then dried in a vacuum oven at  $50\text{ }^\circ\text{C}$  for  $5\text{ h}$  to remove the solvent. The sample surfaces were later gold-coated and examined by scanning electron microscopy. The AFM was also used to visualize the surface topology at room temperature. A nano-sensor cantilever (i.e., the NCL-R type) with a typical static load of  $10\text{ nN}$  and dynamic frequency of  $190\text{ kHz}$  was used. The samples were first cut with a metal knife in cryogenic condition at  $-100\text{ }^\circ\text{C}$  to obtain a smooth surface before examining by AFM.

## Results and discussion

### Mixing torque and temperature

The mixing torque–time curves of ADS/TPU and ENR-50/TPU simple blends with 30/70 and 40/60 compositions are shown in Fig. 1. It can be seen that the blends show two sharp peaks. The first peak at a mixing time of approximately  $0.5\text{ min}$  is related to the incorporation of un-melt rubber mix into the mixing chamber. A decrease in mixing torque is then observed due to the melting of rubber material and again it increases sharply at a mixing time of approximately  $1.2\text{--}1.4\text{ min}$ . This is due to the viscosity of the blends after incorporation of TPU into the mixing chamber. Then, the mixing torque decreases abruptly until the mixing time of approximately  $1.5\text{ min}$  due to the melting of TPU. Thereafter, a gradual decrease in torque is observed until the mixing time of approximately  $3.5\text{ min}$  and becomes almost constant. In Fig. 1, it is also seen that the ENR blends exhibited higher mixing torque relative to that of the ADS blends. This may be attributed to higher chemical interaction between the polar functional groups present in ENR and TPU molecules. The possible chemical interaction is as shown in Scheme 1. This interaction creates stronger links between the surfaces of the two materials or at the interfaces. This may cause an increasing trend of mixing torques. Furthermore, it can be seen that the mixing torque of the blends increased with proportional increase of NR. This is attributed to the higher shear viscosity of pure rubber (i.e., ADS and ENR-50) compared to pure TPU, as also confirmed in Fig. 3.

Figure 2 shows the mixing temperature–time curves of the blends with various types and different proportions of NR. It is seen that the mixing temperature is decreased

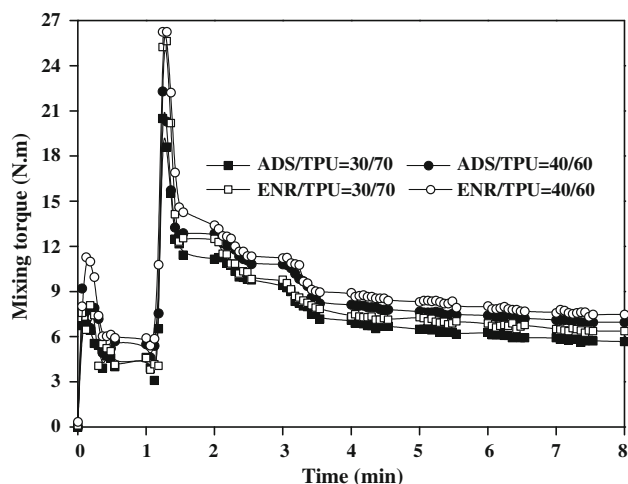
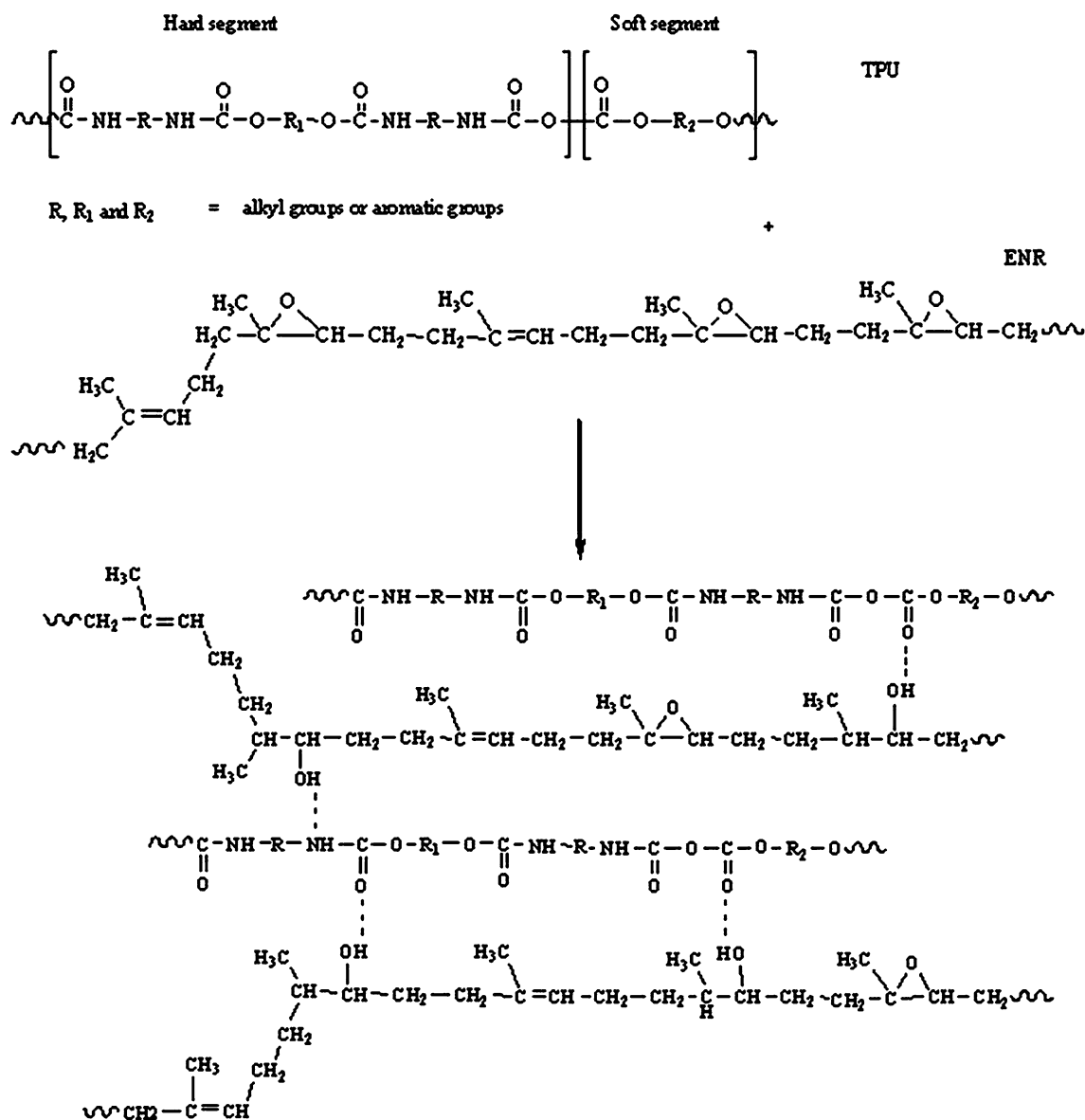


**Fig. 1** Relationship between mixing torque–time of 30/70 and 40/60 ADS/TPU and ENR-50/TPU simple blends



**Scheme 1** Possible chemical interaction between polar functional groups of TPU and ENR

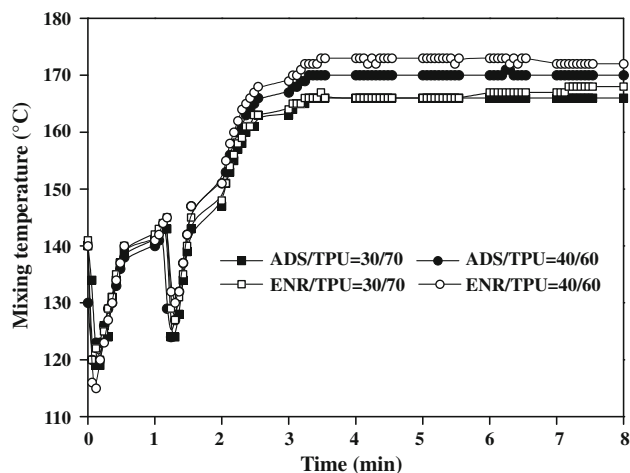
after the addition of rubber mix into the mixing chamber due to the initial temperature of the mix. The mixing temperature is then increased to 140–145 °C by the incorporation of the TPU component. A sharp and immediate decrease in mixing temperature is noticed due to the initial temperature of TPU and again an abrupt increase with the mixing time until approximately 3 min. Then, plateau zones of mixing temperature are observed in the temperature range of 166–175 °C until the mixing time of 8 min. In Fig. 2, it is also seen that the blends with ENR exhibit a higher final mixing temperature compared to the ADS blends. This might be attributed to the higher frictional heat generated from higher chemical interaction between polar functional groups of ENR and TPU molecules. Additionally, it is seen that the final mixing

temperature of the blends increases with the loading level of rubber. This is due to the fact that higher proportion of rubber causes higher shear viscosity of the blend system. This leads to the generation of higher mixing torque (Fig. 1) and frictional heat during the blending operation.

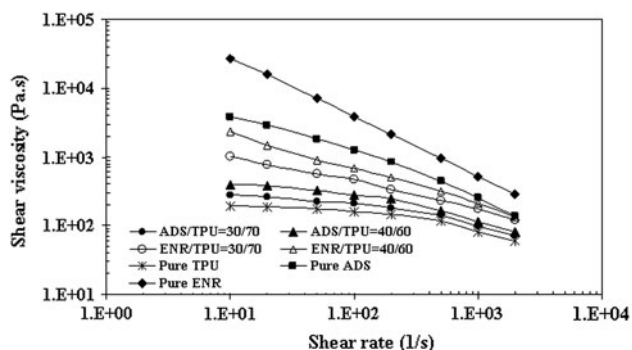
#### Rheological property

Figure 3 shows the relationship between apparent shear viscosity and apparent shear rate (i.e., viscosity curves) of pure TPU, ADS and ENR, and also the simple blends of ADS/TPU and ENR-50/TPU with 30/70 and 40/60 compositions. It can be seen that shear-thinning behavior is observed for all types of materials. That is, the shear viscosity is decreased with increasing shear rate. Furthermore, it is seen that pure ENR





**Fig. 2** Relationship between mixing temperature–time of 30/70 and 40/60 ADS/TPU and ENR-50/TPU simple blends



**Fig. 3** Relationship between apparent shear viscosity and apparent shear rate of pure TPU, pure ADS, pure ENR and 30/70 and 40/60 ADS/TPU and ENR-50/TPU simple blends

exhibits the highest shear viscosity followed by pure ADS and pure TPU, respectively. This corresponds to the higher intermolecular forces between the polar functional groups (i.e., epoxide groups) in ENR molecules together with higher possibility of chain entanglement of longer molecular chains. However, the TPU contains a number of polar functional groups including ester groups in soft domains and urethane groups in hard crystalline domains, which should exhibit a higher viscosity curve. As a matter of fact, during melting of TPU, the crystalline regions disappear and transform to the amorphous phase. Also, TPU contains much lower molecular mass compared to ADS and ENR. Hence, lower flow resistance is observed in the molten TPU even at higher level of chemical interaction between the chains. Therefore, it is concluded that much longer molecular chains with higher degree of chain entanglement of ADS and ENR are responsible for higher flow resistance or apparent shear viscosity. In Fig. 3, higher viscosity curves are also observed in the blends of ENR. This is attributed to the higher chemical interaction between the polar groups of ENR and TPU together with

higher degree of chain entanglement of the ENR molecules. This result corresponds to the higher final mixing torque in Fig. 1. Moreover, it is also seen that the shear viscosity of the blends increased with increasing proportion of NR, which corresponds to the higher final mixing torques (Fig. 1) and shear viscosity of rubber (i.e., ADS and ENR) compared to that of pure TPU.

### Mechanical properties

The stress–strain curves of pure TPU and the blends with different types and proportions of NR are shown in Fig. 4. It is clearly seen that the incorporation of rubber lowers the stress–strain curves by depressing the mechanical properties (i.e., moduli, tensile strength and elongation at break) of the blends compared to the pure TPU, as summarized in Table 1. However, in this study, the main aim was to prepare low hardness TPU materials with good damping properties and acceptable mechanical strength for some applications. Therefore, strength is not the first priority and the reduction can be tolerated. In Fig. 4, it is also seen that the blends with ENR exhibited higher initial slope of the curve (i.e., Young's modulus) than the ADS blends. Furthermore, the Young's modulus decreased with increasing proportion of ENR in the

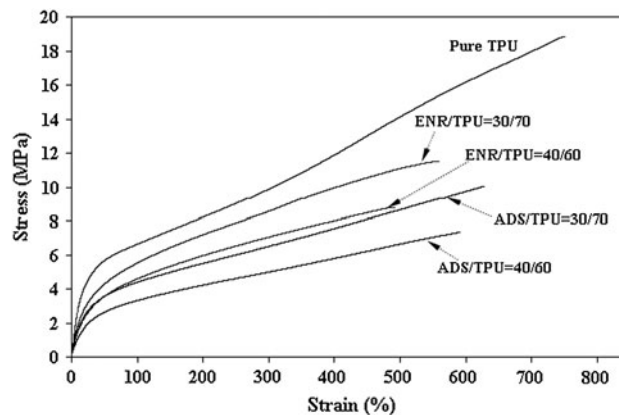


**Fig. 4** Stress–strain curves of pure TPU, 30/70 and 40/60 ADS/TPU and ENR-50/TPU simple blends

**Table 1** Mechanical properties of pure TPU, ADS/TPU and ENR-50/TPU simple blends

Sample	100% modulus (MPa)	200% modulus (MPa)	Tensile strength (MPa)	Elongation at break (%)
Pure TPU	7.3	9.3	18.9	753.3
ADS/TPU (30/70)	4.3	5.5	10.1	629.0
ADS/TPU (40/60)	3.2	4.1	7.3	593.0
ENR/TPU (30/70)	5.5	7.2	11.5	560.0
ENR/TPU (40/60)	4.6	6.0	8.8	494.0



blends. This corresponds to a lower stiffness and hence higher softness of the material with higher content of rubber in the blends. In Table 1, it is also seen that ENR/TPU blends exhibited higher tensile strength and moduli, but lower elongation at break relative to those of the ADS/TPU blends. This may be due to the chemical interaction between the polar functional groups in the ENR molecules and the polar functional groups in the polyester and polyurethane segments in TPU molecules, which also corresponds to higher mixing torque (Fig. 1) and apparent viscosity (Fig. 3) of the ENR/TPU blends. However, it is clear that the moduli and tensile strength of the blends decreased with increasing proportion of ADS and ENR. Therefore, the incorporation of NR shows reduction in stiffness (i.e., Young's modulus) and hence hardness properties of the material, as shown in Fig. 5. Furthermore, in Fig. 5, it is seen that the incorporation of NR results in marked decrease in tension set, which indicates the improvement of elasticity or tendency to recover the original shape after a prolonged deformation. In addition, a lower tension set or higher rubber elasticity is also observed in the blends with higher proportion of NR. Moreover, the blends with ENR show higher tension set values compared to the ADS blends. This is an unexpected result from TPU/ENR blend, which provides higher elasticity and hence lower tension set value due to the chemical interaction between the phases. However, there is a large difference in molecular weight between ADS and ENR molecules, which could be implied by the Mooney viscosity [ML 1 + 4 (100 °C)], and they are 101 for ADS and 70 for ENR-50. Therefore, the influence of longer molecular chains may be more pronounced in controlling the elasticity of the blend system. However, the tension set for all types of blends prepared in this work is lower than 20%. Therefore, the blends with low hardness (i.e., <70 Shore A) and higher elasticity by restraining some levels of mechanical strength have been prepared. Also, it is possible to use these types of materials for some engineering applications.

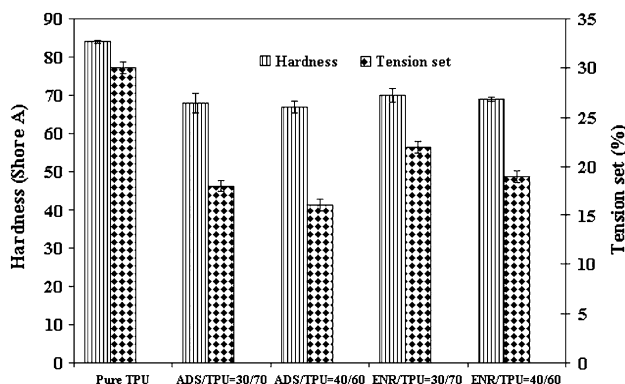
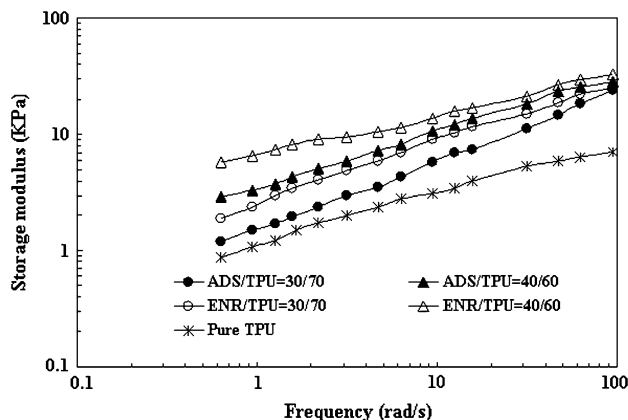


**Fig. 5** Hardness and tension set of pure TPU, 30/70 and 40/60 ADS/TPU and ENR-50/TPU simple blends

## Dynamic mechanical properties

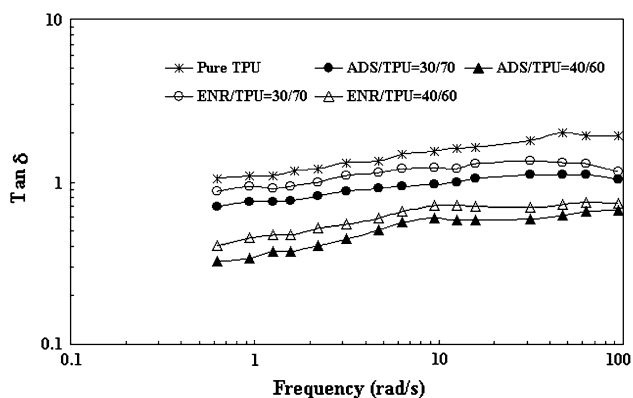
Figure 6 shows the storage or elastic modulus ( $G'$ ) as a function of frequency of pure TPU compared to ADS/TPU ratios of 30/70 and 40/60 and ENR-50/TPU simple blends. The storage or elastic modulus is a measure of the stored energy, representing the elastic portion of the materials. It can be seen that all samples show an increase in storage modulus (or higher stored energy) with increasing oscillating frequency. This may be due to the shorter available time for a molecular relaxation. Furthermore, at a given oscillating frequency, pure TPU exhibited the lowest storage modulus, which implies the lowest capability to store energy and elasticity. In addition, it can be seen that the blends with ENR exhibited higher  $G'$  than that the blends with ADS. This is attributed to the stronger interfacial interaction in ENR/TPU blends. Also, it is clear that increasing proportion of rubber in the blend causes an increase of storage modulus. This is due to the higher content of elastic proportion in the blends. It is also seen that the  $G'$  values of rubber/TPU blends show the same trend as mixing torque (Fig. 1), tensile strength (Table 1) and shear viscosity (Fig. 3). Furthermore, the elastic modulus of the blends increased with increasing blend proportion of rubber, which corresponds to the increasing trend of mixing torque (Fig. 1) and shear viscosity (Fig. 3).

Figure 7 shows the damping factor (i.e.,  $\tan \delta$ ) as a function of oscillating frequency for various proportions of NR/TPU blends with two different types of NR (ADS and ENR).  $\tan \delta$  is the ratio between the loss modulus ( $G''$ ) to the storage modulus ( $G'$ ) or the ratio of viscous to elastic properties (i.e.,  $\tan \delta = G''/G'$ ). It can be seen that at a given oscillating frequency, pure TPU exhibited the highest damping factor, which indicates the highest viscous properties or lowest elastic properties. In Fig. 7, it is clear that the incorporation of NR promotes the enhancement of damping properties of TPU materials. That is, lower  $\tan \delta$  values are observed in the NR/TPU blends. By comparing the blends with different types of



**Fig. 6** Storage modulus as a function of frequency of pure TPU, 30/70 and 40/60 ADS/TPU and ENR-50/TPU simple blends





**Fig. 7** Damping factor ( $\tan \delta$ ) as a function of frequency of pure TPU, 30/70 and 40/60 ADS/TPU and ENR-50/TPU simple blends

rubber, it can be seen that at a given blend proportion and oscillating frequency, the ENR/TPU blends exhibit slightly higher  $\tan \delta$  values than the ADS/TPU blends. This is again an unexpected result as in the case of tension set value of TPU/ENR blend, which provides higher elasticity and hence lower  $\tan \delta$  value due to the chemical interaction between the phases. However, as described earlier, the larger molecules of ADS offer higher elasticity to the blends than the smaller ENR molecules. In Fig. 7, it is also seen that the  $\tan \delta$  of NR/TPU blend with higher rubber content shows lower  $\tan \delta$  or damping factor. This may be related to greater elastic response (i.e., elastomeric properties), which leads to lower  $\tan \delta$ . These results correlate well with lower tension set in Fig. 5.

#### Temperature scanning stress relaxation

Figure 8 shows the normalized force–temperature curves of pure TPU and its blends with ADS and ENR-50. It can be seen that at the beginning stage of the curves (as magnified in the right corner of Fig. 8), force is slightly increased with

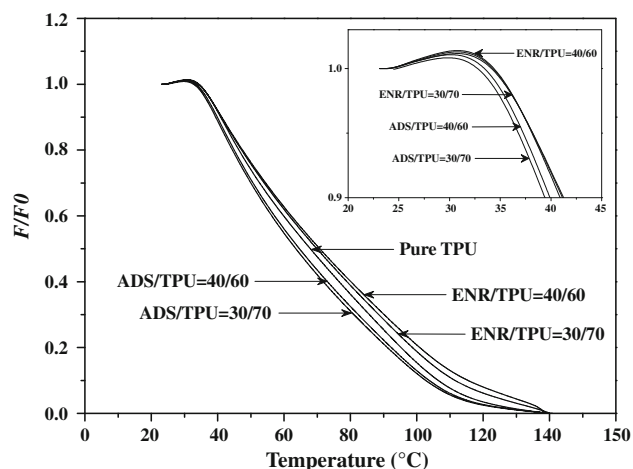


**Fig. 8** Normalized force–temperature curves of pure TPU, 30/70 and 40/60 ADS/TPU and ENR-50/TPU simple blends

**Table 2** TSSR results of pure TPU, ADS/TPU and ENR-50/TPU simple blends

Sample	$F_0$	$T_{10}$	$T_{50}$	$T_{90}$	RI
Pure TPU	3.24	40.9	68.0	106.0	0.58
ADS/TPU (30/70)	1.95	39.4	63.6	102.7	0.57
ADS/TPU (40/60)	1.55	39.9	64.7	103.8	0.56
ENR/TPU (30/70)	2.16	41.2	69.9	111.6	0.57
ENR/TPU (40/60)	1.81	41.3	70.8	115.5	0.56

increasing temperature due to the entropy effect. On further increase in temperature there is stress relaxation, which thereafter overshadows the entropy effect. Therefore, a sudden decreasing trend of force (i.e., stress relaxation) is observed on approaching zero. It is noted that the thermo-oxidative reaction is also one of the main parameters that causes severe stress relaxation. An increase in the initial portion of the curve is related to the level of chain entanglement and chemical interaction between the different phases of the simple blends. However, in vulcanized rubber and thermoplastic vulcanizates (i.e., TPVs), the slope at the initial part of the curve depends on the cross-link density of rubber network [39–41]. In Fig. 8, it is also seen that the blends with ENR showed slightly higher initial slope than that of the blend with ADS. This is attributed to the chemical interaction between the oxirane groups in ENR molecules and polar functional groups in polyester and urethane segments of TPU molecules. As a result of higher compatibility between ENR and TPU, the stress relaxation, thermal resistance and elastomeric nature of the blends are improved. Therefore, it is concluded that the blends with ENR show higher normalized force–temperature curves leading to higher initial force ( $F_0$ ), RI and  $T_x$  values than the blends with ADS, as shown in Table 2. Moreover, the incorporation of ENR is also contributed to improve the thermal resistance of the blend, as shown in Fig. 9. It is seen that the peak of relaxation spectra at

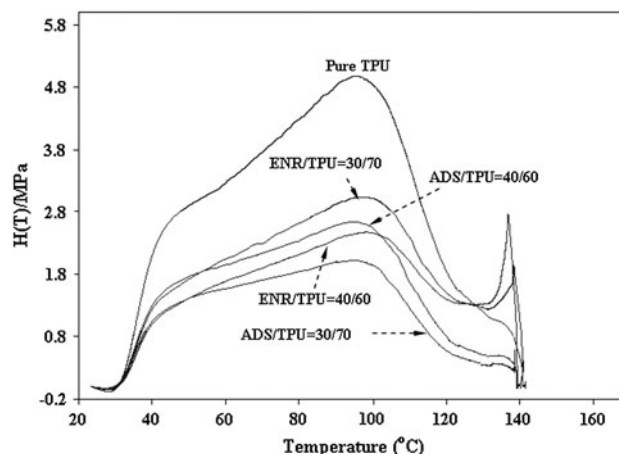


**Fig. 9** TSSR relaxation spectra of pure TPU, 30/70 and 40/60 ADS/TPU and ENR-50/TPU simple blends



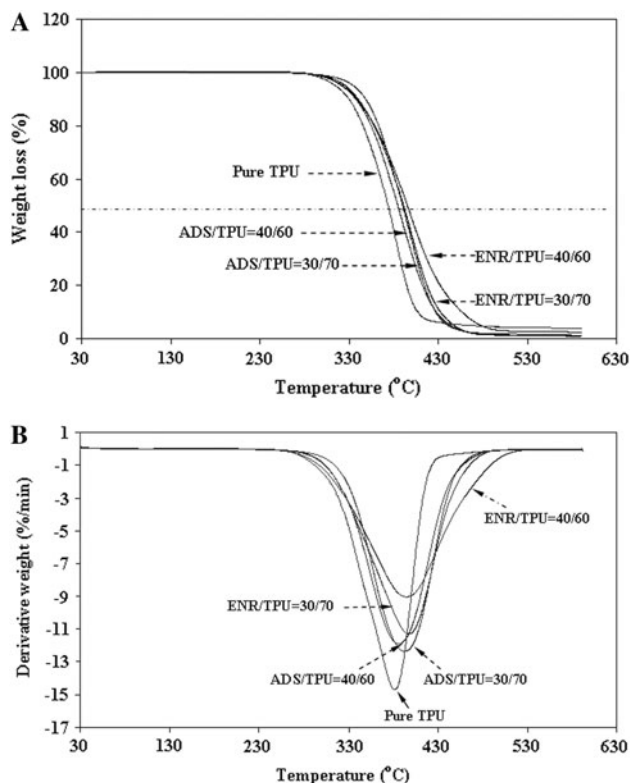


**Fig. 10** TGA (a) and DTG (b) thermograms of pure TPU, 30/70 and 40/60 ADS/TPU and ENR-50/TPU simple blends

approximately 100 °C revealed the thermal resistance of the blends during the TSSR test. That is, the peak of the blends with ENR shifts to higher temperature than that of the ADS blends. The locations of the peaks are correlated well with the values of  $T_{90}$  of the blends (Table 2). This confirms the effective increase in thermal resistance of ENR/TPU blends.

#### Thermal resistant properties

Thermal resistance or thermal stability of NR/TPU blends have been investigated by TGA. Figure 10 shows the TGA and DTG thermograms of ADS/TPU and ENR-50/TPU simple blends with 30/70 and 40/60 compositions. It is seen that all types of blends have exhibited single degradation step with single degradation temperature ( $T_d$ ) estimated from the peak of DTG curves, as summarized in Table 3. The temperatures at 5 and 50% weight losses are also summarized in Table 3. It is clear that the ENR/TPU blends exhibited higher temperature values of  $T_{5\%}$ ,  $T_{50\%}$  and  $T_d$  than the ADS/TPU blends and pure TPU, respectively. This is related to the higher thermal resistance of ENR/TPU blends based on TSSR measurement (Fig. 9), which corresponds to higher  $T_x$  values (Table 2). This might be attributed to the chemical interaction between different phases. Furthermore, intrinsic thermal stability of the parent polymer is another reason for higher thermal

**Table 3** Temperature at which 5 and 50% weight losses occur and degradation temperature ( $T_d$ ) of pure components, ADS/TPU and ENR-50/TPU simple blends

Sample	$T_{5\% \text{ wt}}$ (°C)	$T_{50\% \text{ wt}}$ (°C)	DTG max ( $T_d$ ) (°C)
Pure ADS	332.6	377.1	377.6
Pure ENR	335.7	398.0	405.7
Pure TPU	313.6	370.7	379.0
ADS/TPU (30/70)	330.4	390.0	388.6
ADS/TPU (40/60)	323.0	384.6	394.8
ENR/TPU (30/70)	326.1	391.0	393.7
ENR/TPU (40/60)	328.1	395.3	398.0

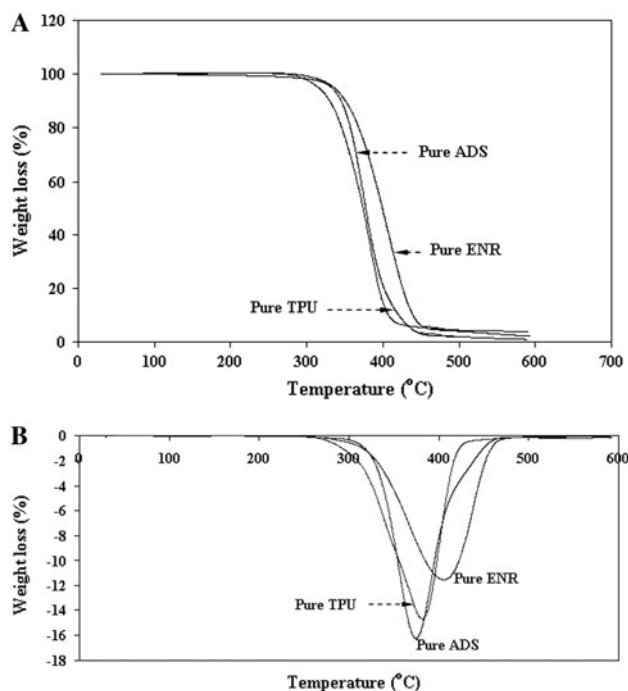


**Fig. 11** TGA (a) and DTG (b) thermograms of pure polymers (ADS, ENR and TPU)

resistance, as shown in TGA and DTG thermograms of pure polymers (Fig. 11). It is seen that the pure ENR exhibited the highest  $T_d$  at approximately 405.7 °C, while the ADS and TPU exhibited lower  $T_d$  at approximately 377.6 and 379.0 °C, respectively. This indicates that, apart from the higher chemical interaction between ENR and TPU phases, higher thermal resistance of pure ENR causes higher  $T_d$  of the ENR/TPU blends than the ADS/TPU blends.

#### Dynamic mechanical analysis

Figure 12 shows the relationship between  $\tan \delta$  and temperature of pure polymers (i.e., ADS, ENR and TPU) and its simple blends based on DMA characterization. The

temperature at the  $\tan \delta$  (damping) peak corresponds to glass transition temperature ( $T_g$ ). Each type of polymer shows an individual peak corresponding to the  $T_g$  values, as shown in Table 4. It can be seen that the pure ADS exhibits the lowest  $T_g$  value at approximately  $-52.2$  °C, while pure ENR shows higher  $T_g$  at approximately  $-11.9$  °C. This indicates the restriction of chain mobility of ENR due to the higher level of intermolecular attraction between epoxirane rings and its product of opened rings along the chains. A sharp intense damping peak appeared at

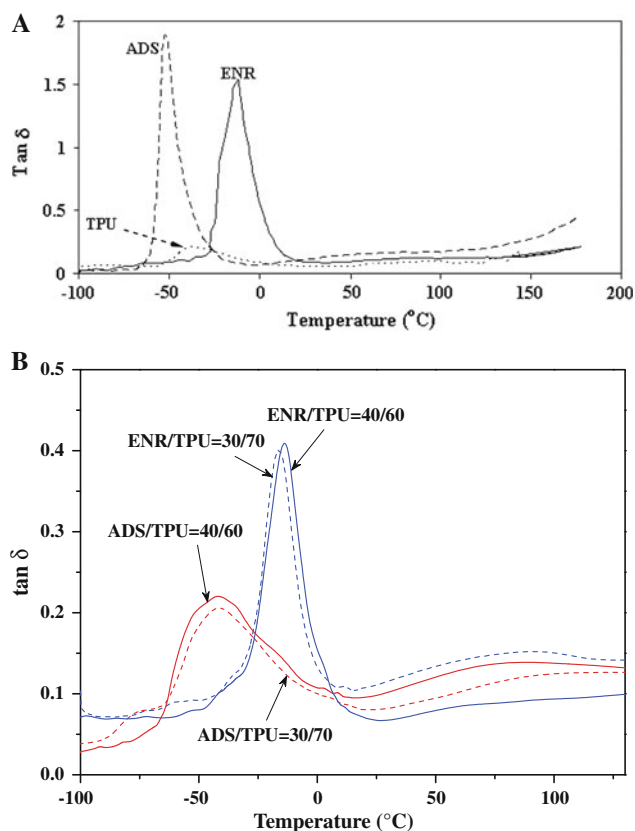


**Fig. 12** Relationship between  $\tan \delta$  and temperature of pure polymer (a), and 30/70 and 40/60 ADS/TPU and ENR-50/TPU simple blends (b) based on DMA characterization

$-35.8$  °C for pure TPU, which corresponds to the glass transition of soft segment of TPU. TPU consists of two phases: soft aliphatic polyester segment and hard polyurethane segment. The  $T_g$  based on the intense peak in Fig. 12a represents the  $T_g$  of amorphous soft segment in TPU molecules. Hard phase polyurethane segment should exhibit  $\tan \delta$  peak at higher temperature. However, in Fig. 12b, the second peak could not be clearly specified in the temperature range of 50–120 °C. In Fig. 12b, it is seen that even NR/TPU blends consist of at least two different soft phases (i.e., soft polyester segments of TPU and soft NR phase) and one hard phase of TPU, but only a single sharp intense peak is observed in the thermograms. This might be due to the close values of  $T_g$  of soft amorphous phase of TPU and two types of NR (i.e., ADS and ENR-50). This causes a shift in  $T_g$  toward other  $T_g$ s and as a result representing a single  $T_g$ , which indicates a significant compatibilization of the blends. It is noted that the  $T_g$  for hard phase of TPU should exist at higher ranges of temperature. However, in Fig. 12b, the  $\tan \delta$  peaks at temperature higher than 50 °C could not be clearly determined. Therefore, in ENR/TPU blends, it is clear that its  $T_g$  is located between  $T_g$  values of pure TPU and pure ENR. This is due to the chemical interaction between the polar functional groups, which causes partial compatibilization of the blends. Meanwhile, the ADS/TPU blends show very similar  $\tan \delta$  curves compared to that of pure TPU curve, and the peak lies between those of pure ADS and pure TPU. However, there may be some poor chemical interactions between these two phases. Therefore, ADS/TPU blend shows almost superimposed or closely separated  $\tan \delta$  peak from the peaks of ADS and TPU. Furthermore, in Fig. 12a it can be seen that the pure NR (i.e., ADS and ENR-50) shows a much larger area below the  $\tan \delta$  curves. A large area under the  $\tan \delta$  curve indicates a great degree of molecular mobility, which translates into better damping properties. In Fig. 12b, a slightly higher area is observed below the  $\tan \delta$  curve of ADS/TPU blend. This indicates a greater degree of chain molecular mobility and superior

**Table 4** Glass transition temperature ( $T_g$ ), crystalline melting temperature ( $T_m$ ) and heat of crystallization of pure components, ADS/TPU and ENR-50/TPU simple blends

Sample	$T_g$ (°C) DMA	$T_g$ (°C) DSC	$T_m$ (soft) (°C)	Heat of crystallization (soft) (J/g)	$T_m$ (hard) (°C)	Heat of crystallization (hard) (J/g)
Pure TPU	-35.8	-51.3	15.3	12.9	135.9	16.5
ADS/TPU (30/70)	-41.6	-66.3	15.1	4.7	132.5	9.7
ADS/TPU (40/60)	-43.1	-66.8	14.9	7.7	133.2	3.6
ENR/TPU (30/70)	-17.2	-29.0	14.5	2.1	132.7	7.8
ENR/TPU (40/60)	-14.4	-29.0	14.0	5.4	132.2	2.4
Pure ADS	-52.1	-66.3	-	-	-	-
Pure ENR	-11.9	-25.9	-	-	-	-



damping properties. This result correlates well with lower tension set value (Fig. 5) and damping factor (Fig. 7).

Differential scanning calorimetry

DSC thermograms of pure polymers (i.e., TPU, ADS and ENR) and simple blends of ADS/TPU and ENR/TPU with different blend ratios are shown in Fig. 13. Table 4 also

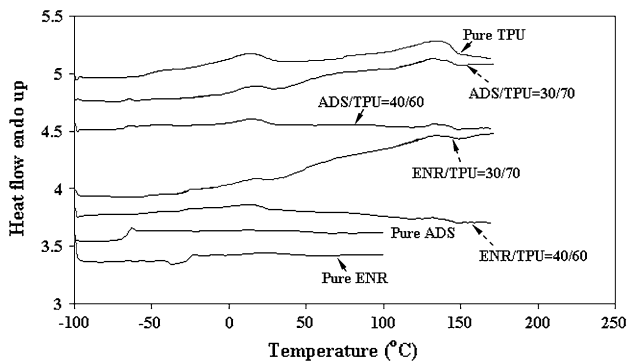
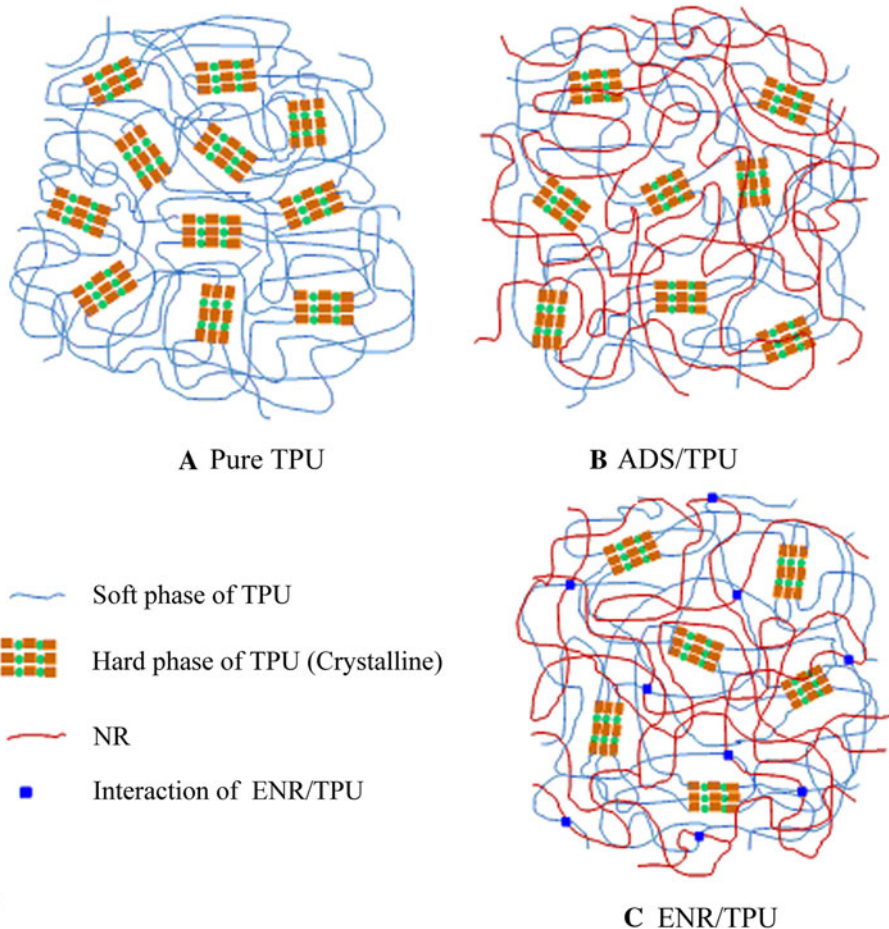
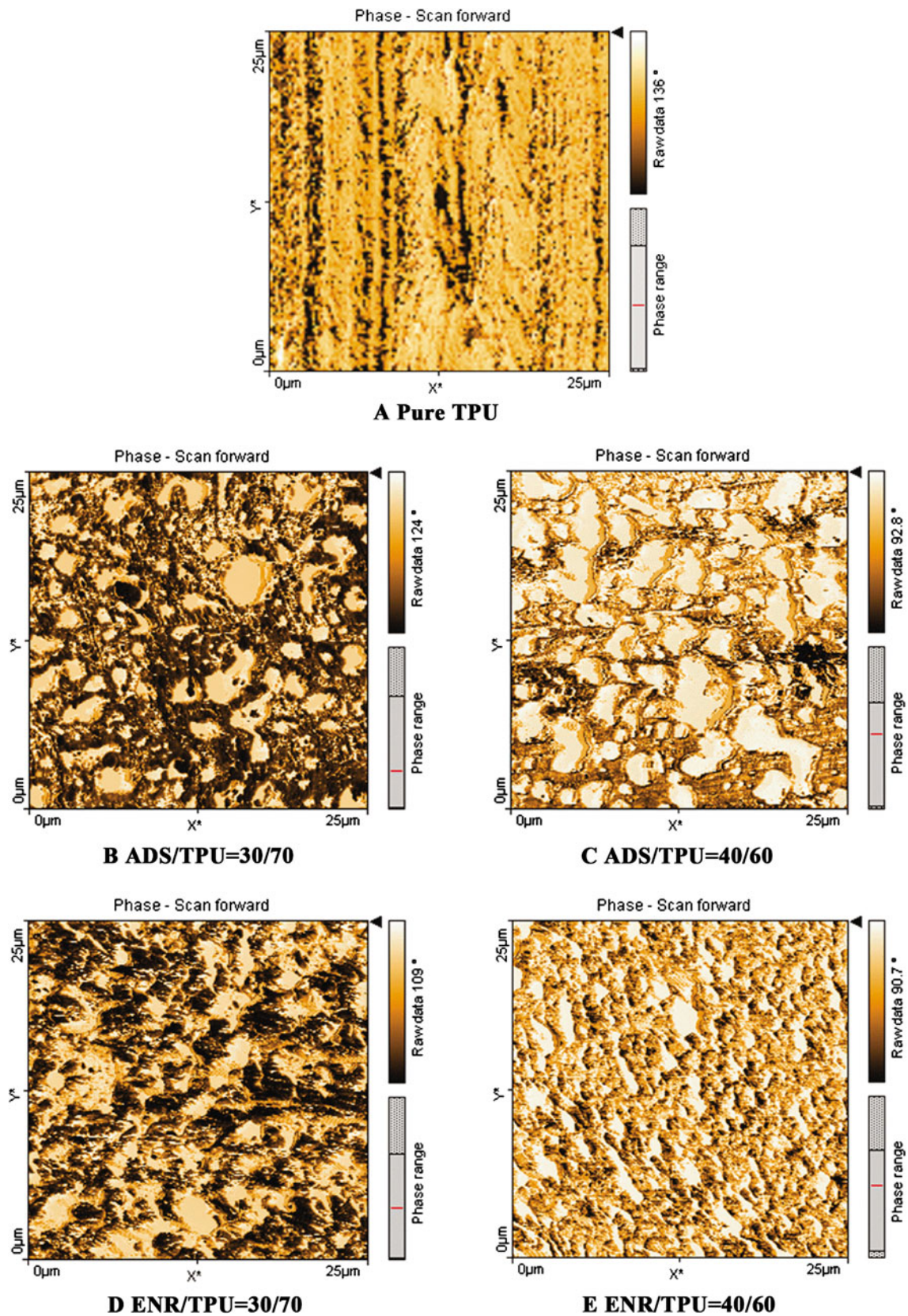


Fig. 13 DSC thermograms of 30/70 and 40/60 ADS/TPU and ENR-50/TPU simple blends and pure TPU, ADS and ENR, respectively

summarizes glass transition temperature ( $T_g$ ), crystalline melting temperature ( $T_m$ ) and heat of crystallization of pure polymer components and the simple blends based on DSC characterization. Pure TPU shows the glass transition temperature ( $T_g$ ) of soft segment at approximately  $-51.3\text{ }^\circ\text{C}$ , while the  $T_g$  of ADS and ENR are observed at  $-66.3$  and  $-25.9\text{ }^\circ\text{C}$ , respectively. It is noted that the  $T_g$ s based on DSC are different compared to the  $T_g$ s characterized by DMA. This is attributed to different evaluation methods adopted in  $T_g$  measurement. That is, DSC quantified  $T_g$  is based on the enthalpy change, while the mechanical treatment is exploited in DMA characterization method. In Fig. 13, it is also seen that the NR/TPU blends show a single  $T_g$  lying between the  $T_g$ s of rubber and soft segments of pure TPU. It has been well established that the structure of TPU consists of two segments of hard and soft domains. The TPU used in this work is capable of partial crystallization. Therefore, two melting temperatures are observed in the DSC thermograms of pure TPU and NR/TPU blends. First melting temperature of pure TPU represents melting of regular domains in soft segments of TPU (i.e.,  $T_m$  (soft)) in the range of  $14.2\text{--}15.4\text{ }^\circ\text{C}$ . The other melting temperature range of  $132.2\text{--}135.9\text{ }^\circ\text{C}$  indicates the

Fig. 14 Schematic illustrating crystallization of TPU phase in ADS/TPU and ENR/TPU simple blends based on: (a) pure TPU, (b) ADS/TPU and (c) ENR/TPU blends





**Fig. 15** AFM micrographs of pure TPU and 30/70 and 40/60 ADS/TPU and ENR-50/TPU simple blends



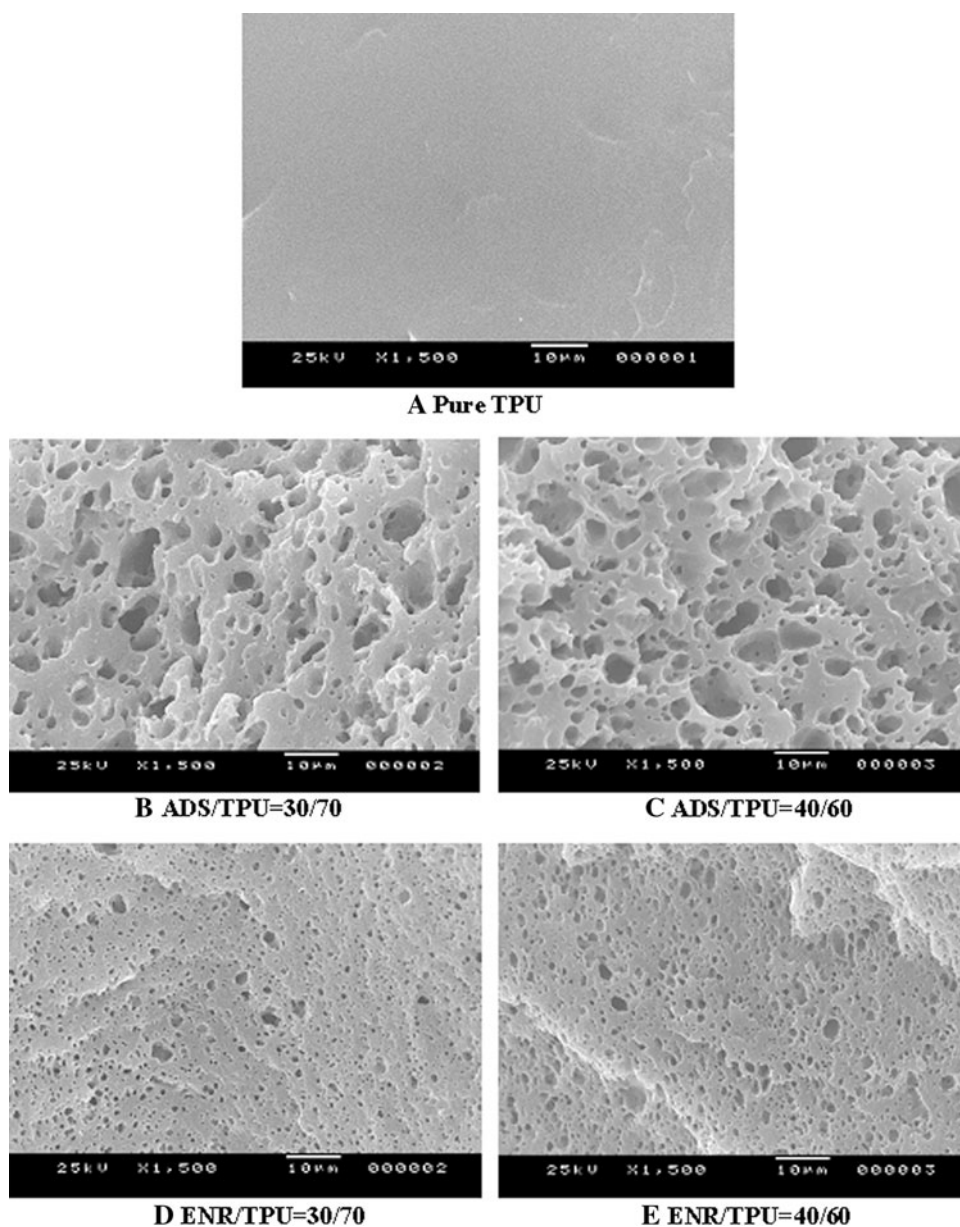
melting of hard polyurethane domains in TPU molecules (i.e.,  $T_m$  for hard segment). From Fig. 13 and Table 4, it is also seen that the incorporation of NR reduces  $T_m$  and heat of crystallization of TPU hard phase. That is, disruption of regular crystalline segments occurs due to the higher shearing force during mixing operation with NR. Furthermore, it is also seen that ENR blends exhibit lower  $T_m$  and heat of crystallization than that of ADS. This is attributed to higher chemical interaction between the polar functional groups of ENR and TPU molecules. This may be due to lower degree of crystallinity, as shown schematically in a diagram in Fig. 14. In Fig. 13, lower  $T_m$  and heat of crystallization of NR/TPU blends is observed with higher rubber content, which directly corresponds to the lower

degree of crystallinity. This is related to the interference of rubber phases on the formation of regular crystalline phase of TPU after melting during blending operation.

#### Morphological properties

Figure 15 shows the AFM micrographs of pure TPU and the simple blends of ADS/TPU and ENR-50/TPU with different compositions. It is seen that the pure TPU shows regular crystalline regions (black spots), which act as hard phase and tie points for aliphatic polyester soft segments. Blending of NR and TPU changes the morphological properties dramatically. That is, more black regions are observed in 30/70 ADS/TPU and ENR/TPU blends with

**Fig. 16** SEM micrographs of pure TPU and 30/70 and 40/60 ADS/TPU and ENR-50/TPU simple blends



lower proportion of rubber. The higher proportions of rubber have helped the disappearance of some crystalline hard phase, as indicated in Table 4. This may be due to the influence of mixing operation at high shearing action and high temperature together with the steric hindrance or higher chain entanglement caused by the incorporation of NR in the TPU system. By comparing ADS/TPU and ENR/TPU blends, it is clear that the ENR/TPU blend exhibits finer grain morphology than the ADS/TPU blends, in particular at higher rubber proportion with a blend ratio of 40/60. This is attributed to higher chemical interactions between the phases of ENR and TPU. Furthermore, in AFM images of the simple blends, a difference can be clearly distinguished between the soft phase (i.e., the non-crystalline region of TPU and ENR phase) and hard phase of crystalline regions of TPU. However, no difference could be distinguished between the non-crystalline soft region of aliphatic polyester in the TPU molecules and NR phase in the light yellow regions. Therefore, morphological properties of the NR/TPU simple blends are further investigated by the SEM technique. That is, the rubber phase is first etched from the sample surface by extracting with toluene before examining by SEM. The SEM micrographs are shown in Fig. 16. It can be seen that the pure TPU showed a smooth surface because it could not be extracted by toluene, while the simple blends of ADS/TPU and ENR/TPU with blend ratio of 30/70 exhibited dispersion of ADS or ENR droplets in the TPU matrix, where larger ADS droplets were observed compared to the ENR droplets. This is attributed to higher interfacial interaction in ENR/TPU blends and lower Mooney viscosity of ENR relative to ADS. However, in the simple blends of ADS/TPU with a blend ratio of 40/60, a co-continuous structure is observed, while the ENR/TPU exhibits sea-island morphology with finer grain morphology due to higher blend compatibility and lower Mooney viscosity of the ENR. This correlates well with higher moduli, tensile strength (Table 1),  $T_{10}$ ,  $T_{50}$ ,  $T_{90}$  and RI (Table 2), degradation temperature (Table 3), mixing torque (Fig. 1), mixing temperature (Fig. 2), viscosity curve (Fig. 3) and Young's modulus (Fig. 4).

## Conclusion

NR/TPU blends were prepared using two types of NR: ADS and ENR-50. The main aim of this study was to prepare low hardness TPU material with higher thermal resistance, superior elastic properties and low damping factor. It was found that ENR/TPU blends exhibited higher mixing torque, Young's modulus, tensile strength and thermal degradation compared to ADS/TPU blends. However, inferior damping property ( $\tan \delta$ ), elongation at break

and elasticity in terms of tension set properties were observed in ENR/TPU blends. This can be ascribed to ADS having contained rather large molecules which imparted higher elasticity to the blends. It was also found that ENR/TPU blends gave higher stress relaxation behavior, thermal resistance and thermal degradation than the ADS/TPU blends. Increase in rubber content resulted in enhancement of mixing torque, apparent shear viscosity and coarse grain morphology of the blends. However, Young's modulus, tensile strength, elongation at break, hardness, tension set, damping properties and  $T_g$  of the blends were decreased. Therefore, it is concluded that the TPU materials with low hardness (i.e., <70 Shore A) and higher elasticity (i.e., lower tension set and  $\tan \delta$ ) by restraining some levels of mechanical strength have been prepared and can be used for some industrial applications.

**Acknowledgments** The authors gratefully acknowledge the Thailand Research Fund through the Royal Golden Jubilee Ph.D. Program (Grant no. PHD/0101/2550), University of Applied Science, Osnabrück, Germany and the National Research University Project of Thailand's Office of the Higher Education Commission for financial support.

## References

1. Ibrahim A, Dahlan M (1998) Thermoplastic natural rubber blends. *Prog Polym Sci* 23:665–706
2. Rader CP (2003) Thermoplastic elastomer. In: Del Vecchio RJ (ed) *Fundamental of rubber technology: a pragmatic in-depth introduction to the compounding and processing of rubber*. Rubber Division
3. Nakason C, Jamjinno S, Kaesaman A, Kiatkamjornwong S (2008) Thermoplastic elastomer based on high-density polyethylene/natural rubber blends: rheological, thermal, and morphological properties. *Polym Adv* 12:85–98
4. Dahlan HM, Khairul Zaman MD, Ibrahim A (2002) The morphology and thermal properties of liquid natural rubber (LNR)-compatibilized 60/40 NR/LLDPE blends. *Polym Test* 21:905–911
5. Thitithammawong A, Nakason C, Sahakaro K, Noordermeer JWM (2007) NR/PP thermoplastic vulcanizates: selection of optimal peroxide type and concentration in relation to mixing conditions. *J App Polym Sci* 106:2204–2209
6. Asaletha R, Bindu P, Aravind I, Meera AP, Valsaraj SV, Yang W, Thomas S (2008) Stress-relaxation behavior of natural rubber/polystyrene and natural rubber/polystyrene/natural rubber-graft-polystyrene blends. *J Appl Polym Sci* 108:904–913
7. Mina MF, Ania F, Balta Calleja FJ, Asano T (2004) Microhardness studies of PMMA/natural rubber blends. *J Appl Polym Sci* 91:205–210
8. Nakason C, Jarntong M, Kaesaman A, Kiatkamjornwong S (2009) Influences of blend proportions, curing systems on dynamic, mechanical, and morphological properties of dynamically cured epoxidized natural rubber/high-density polyethylene blends. *Polym Eng Sci* 49:281–292
9. Nakason C, Jarntong M, Kaesaman A, Kiatkamjornwong S (2008) Thermoplastic elastomers based on epoxidized natural rubber, high-density polyethylene blends: effect of blend compatibilizers on the mechanical and morphological properties. *J Appl Polym Sci* 109:2694–2702

10. Thitithammawong A, Nakason C, Sahakaro K, Noordermeer JWM (2007) Effect of different types of peroxides on rheological, mechanical, and morphological properties of thermoplastic vulcanizates based on natural rubber/polypropylene blends. *Polym Test* 26:537–546
11. Nakason C, Wannavilai P, Kaesaman A (2006) Thermoplastic vulcanizates based on epoxidized natural rubber/polypropylene blends: effect of compatibilizers and reactive blending. *J Appl Polym Sci* 100:4729–4740
12. Mohamad Z, Ismail H, Thevy RC (2006) Characterization of epoxidized natural rubber/ethylene vinyl acetate (ENR-50/EVA) blend: effect of blend ratio. *J Appl Polym Sci* 99:1504–1515
13. Mousa A, Ishiaku US, Mohd Ishak ZA (2000) Rheological properties of dynamically vulcanized poly(vinyl chloride)/epoxidized natural rubber thermoplastic elastomers: effect of processing variables. *Polym Test* 19:193–204
14. Nakason C, Tobprakhon A, Kaesaman A (2005) Thermoplastic vulcanizates based on poly(methyl methacrylate)/epoxidized natural rubber blends: mechanical, thermal, and morphological properties. *J Appl Polym Sci* 98:1251–1261
15. Nakason C, Panklieng P, Kaesaman A (2004) Rheological and thermal properties of thermoplastic natural rubbers based on poly(methyl methacrylate)/epoxidized-natural-rubber blends. *J Appl Polym Sci* 92:3561–3572
16. Khosrokhavar R, Naderi G, Bakhshandeh GR, Ghoreishy MHR (2011) Effect of processing parameters on PP/EPDM/organoclay nanocomposites using Taguchi analysis method. *Iran Polym J* 20:41–53
17. Gong L, Yin B, Li L-P, Yang M-B (2012) Morphology and properties of PP/EPDM binary blends and PP/EPDM/nano-CaCO<sub>3</sub> ternary blends. *J Appl Polym Sci* 123:510–519
18. Ehsani M, Zeynali ME, Abtahi M, Harati AA (2009) LDPE/EPDM blends as electrical insulators with unique surface, electrical and mechanical properties. *Iran Polym J* 18:37–47
19. Li H, Wang L, Song G, Gu Z, Li P, Zhang C, Gao L (2010) Study of NBR/PVC/OMMT nanocomposites prepared by mechanical blending. *Iran Polym J* 19:39–46
20. Mansour SA, Al-ghoury ME, Shalaan E, El Eraki MHI, Abdel-Bary EM (2011) Dielectric dispersion and AC conductivity of acrylonitrile butadiene rubber-poly(vinyl chloride)/graphite composite. *J Appl Polym Sci* 122:1226–1235
21. Wikipedia (2011) Thermoplastic polyurethane, the Free Encyclopedia, Wikimedia Foundation. Available online: <http://en.wikipedia.org>
22. Holden G, Kricheldorf HR, Quirk RP (1996) Thermoplastic elastomers, 3rd edn. Hanser, Munich, Ch 2
23. Bajsic EG, Pustak A, Smit I, Leskovic M (2010) Blends of thermoplastic polyurethane and polypropylene. II. Thermal and morphological behavior. *J Appl Polym Sci* 117:1378–1834
24. Bajsic EG, Smit I, Leskovic M (2007) Blends of thermoplastic polyurethane and polypropylene. I. Mechanical and phase behavior. *J Appl Polym Sci* 104:3980–3985
25. Ajili SH, Ebrahimi NG, Khorasani MT (2003) Study on thermoplastic polyurethane/polypropylene (TPU/PP) blend as a blood bag material. *J Appl Polym Sci* 89:2496–2501
26. Lu Q, Macosko CW (2004) Comparing the compatibility of various functionalized polypropylenes with thermoplastic polyurethane (TPU). *Polymer* 45:1981–1991
27. Pesetskii SS, Fedorov VD, Jurkowski B, Polosmak ND (1999) Blends of thermoplastic polyurethanes and polyamide 12: structure, molecular interactions, relaxation, and mechanical properties. *J Appl Polym Sci* 74:1054–1070
28. Zhang S, Wang G, Jiang Z, Wang D, Ma R, Wu Z (2005) Impact properties, phase structure, compatibility, and fracture morphology of polyamide-1010/thermoplastic poly(ester urethane) elastomer blends. *J Polym Sci, Part B: Polym Phys* 43:1177–1185
29. Palanivelu K, Sivaraman P, Reddy MD (2002) Studies on thermoplastic polyurethane toughened poly(butylene terephthalate) blends. *Polym Test* 21:345–351
30. Ma H, Yang Y (2008) Rheology, morphology and mechanical properties of compatibilized poly(vinylidene fluoride) (PVDF)/thermoplastic polyurethane (TPU) blends. *Polym Test* 27:441–446
31. Pita VJRR, Sampaio EEM, Monteio EEC (2002) Mechanical properties evaluation of PVC/plasticizers and PVC/thermoplastic polyurethane blends from extrusion processing. *Polym Test* 21:545–550
32. Parnell S, Min K (2005) Reactive blending of thermoplastic polyurethane in situ with poly(vinyl chloride). *Polym Eng Sci* 45:876–887
33. Pötschke P, Wallheinke K, Stutz H (1999) Blends of thermoplastic polyurethane and maleic-anhydride grafted polyethylene. I. Morphology and mechanical properties. *Polym Eng Sci* 39:1035–1048
34. Ulcnik-Krump M (2006) Study of morphology influence on rheological properties of compatibilized TPU/SAN blends. *J Appl Polym Sci* 100:2303–2316
35. Ulcnik-Krump M, De Lucca Freitas L (2004) The study of morphology, thermal and thermo-mechanical properties of compatibilized TPU/SAN blends. *Polym Eng Sci* 44:838–852
36. Pichaiyut S, Nakason C, Kummerlöwe C, Vennemann N (2011) Thermoplastic elastomer based on epoxidized natural rubber/thermoplastic polyurethane blends: influence of blending technique. *Polym Adv Technol*. Available on-line
37. Nakason C, Wannavilai P, Kaesaman A (2006) Effect of vulcanization system on properties of thermoplastic vulcanizates based on epoxidized natural rubber/polypropylene blends. *Polym Test* 25:34–41
38. Cogswell FN (1981) Polymer melt rheology: a guide for industrial practice, vol 24. Woodhead, Cambridge
39. Vennemann N, Bökamp K, Broeker D (2006) Crosslink density of peroxide cured TPV. *Macromol Symp* 245:641–650
40. Barbe A, Bökamp K, Kummerlöwe C, Sollmann H, Vennemann N (2005) Investigation of modified SEBS-based thermoplastic elastomers by temperature scanning stress relaxation measurements. *Polym Eng Sci* 45:1498–1507
41. Narathichat M, Kummerlöwe C, Vennemann N, Nakason C (2011) Thermoplastic natural rubber based on polyamide-12: influence of blending technique and type of rubber on temperature scanning stress relaxation and other related properties. *J Appl Polym Sci* 121:805–814

